Intelligent defect detection in electroluminescence images of photovoltaic modules using MobileNetV2

Inasse Benjelloul [1*], *Hicham* Bouali[1]

[1]Laboratory of Materials, Waves, Energy and Environment, Faculty of Sciences, Mohammed First University, Oujda, Morocco

Abstract. With the rapid growth of the photovoltaic (PV) industry, fast and accurate defect-detection techniques are becoming increasingly important. Manual inspection of PV modules using electroluminescence (EL) imaging is time-consuming and prone to errors. This study proposes a clever method for detecting defects using a lightweight deep learning model based on the MobileNetV2 architecture. The model learns from a dataset of EL images showing two common types of defects: cracks and dark areas. It also contains defect-free cells. To improve robustness to typical EL acquisition variability, an EL-tailored data augmentation pipeline is applied, including geometric transformations and photometric adjustments (brightness and contrast). During testing, it takes only 0.913 seconds to predict an image. This demonstrates a good compromise between speed and accuracy. This approach offers a promising solution for low-cost, near-real-time quality inspection of photovoltaic modules using artificial intelligence.

Keywords: *Photovoltaic modules (PV), electroluminescence imaging (EL), defect detection, deep learning, MobileNetV2*.

1 Introduction

Photovoltaic technology has become a key component of the global energy transition, yet its performance and reliability are strongly influenced by manufacturing imperfections and in-field degradation [1-2]. However, local defects are common in solar cells because they are composed of small particles and their manufacturing process significantly degrades the spatial uniformity and overall conversion efficiency of solar cells [3].

The photovoltaic (PV) industry encompasses a wide range of solar panel technologies, with crystalline silicon (c-Si) cells dominating the market. These cells are manufactured in two main forms: monocrystalline and polycrystalline. Both types exhibit reliable energy conversion efficiencies, typically ranging from 20% to 25%. Due to their mature fabrication processes and favorable cost-to-performance ratio, (c -Si) cells account for approximately 97% of the global PV market. However, various defects may occur in these modules, including (a) malfunctions such as microcracks, finger interruptions and dislocations; (b) assembly defects, including welding errors, and rolling imperfections; and (c) defects resulting from transport and field operations, such as cracks and fractures. Defects can significantly impair the electrical performance of photovoltaic modules, necessitating the creation of effective diagnostic tools for defect detection and categorisation [4-5]. Several methods are used to assess the operational status of photovoltaic modules, including current-voltage IV testing, thermal/infrared IR imaging, leakage current testing, and electroluminescence EL imaging. Although current-voltage IV testing provides an overall assessment of module performance, it lacks the spatial resolution necessary to detect localised problems such as microcracks or interruptions [6]. IR imaging utilizes thermal cameras to identify temperature variations between healthy and defective regions, offering a non-invasive means of fault localization [7]. This method has proven to be a high-resolution approach for detecting a wide range of photovoltaic defects, including cracks and finger interconnects. Thanks to its high sensitivity, EL imaging can be performed in a dark chamber to ensure isolation of the emitted radiation from ambient radiation, including interconnections and short circuits (Fig. 1). It is also possible to conduct it outside in low light (Fig. 2) [8-9]. Testing with EL lets you find hidden flaws in the construction of PV cells without damaging them. It gives a lot of information on how uniform the surface of the solar module is. Even while there are benefits, looking at EL pictures by hand is still hard, takes a lot of time, and can be biased, especially when it comes to making a lot of photovoltaic modules. As a result, there is a rising need for automated and smart methods that can quickly and accurately analyze EL pictures. Recent developments in deep learning, especially in convolutional neural networks (CNNs), have shown great promise for use in picture categorization and defect identification [4-9].

* Corresponding author: inasse.benjelloul@ump.ac.ma

This study presents an intelligent defect detection method utilizing the MobileNetV2 architecture, a lightweight convolutional neural network model optimized for efficient and rapid inference [10]. The model is trained on a labeled EL image dataset comprising both defective and non-defective cells. Data augmentation and transfer learning techniques are employed to enhance generalization from a small dataset [12-3] The efficacy of the proposed method is assessed based on classification accuracy and inference speed, underscoring its suitability for real-time quality inspection in photovoltaic production settings.

2 EL imaging of the PV modules

2.1 EL imaging

Electroluminescence imaging is a non-destructive technique that visualizes electrically active regions of PV cells. When a forward bias is applied, radiative recombination produces near-infrared emission that can be captured by a sensitive camera to form an EL image. In practice, acquisition is often performed under reduced ambient illumination (dark chamber) to maximize contrast and facilitate the detection of subtle defects (Fig. 1) [13-14].

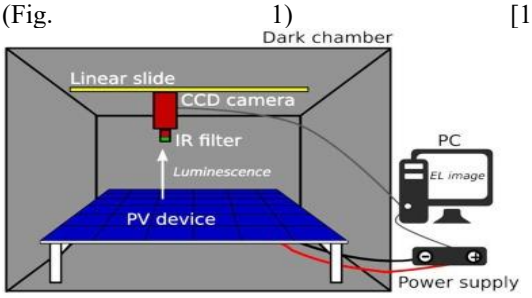

Fig. 1. EL imaging setup in a dark chamber **[9]**.

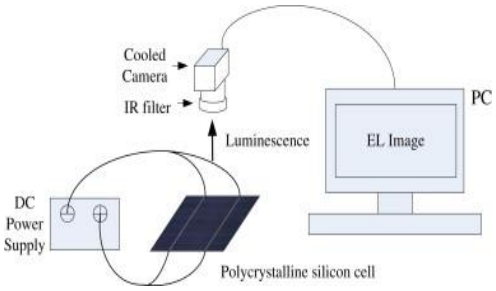

Fig. 2. EL imaging setup **[8]**.

2.2 Detected EL images

This subsection describes the different categories of defects and crack patterns observable in photovoltaic modules using electroluminescence (EL) imaging. Illustrative EL images are shown in (Fig. 3), chosen at random from the ELPV dataset. Identifiable defects include cracks, microcracks, contact breaks, scratches, disconnected cells, diode failures, soldering imperfections, black cores, dark areas, and other anomalies. These anomalies can have a profound impact on the normal functioning of photovoltaic cells, potentially leading to hot spots, significant power loss, or even total failure [14]. Consequently, the development of automated methods for defect detection and classification based on electroluminescence (EL) imaging systems is becoming increasingly necessary.

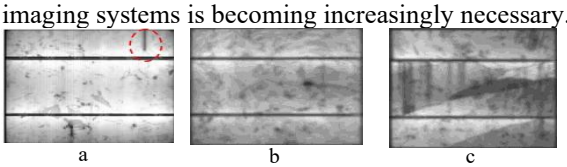

Fig. 3. Defects detectable EL images of mcSi modules (a) finger interruptions, (b) dark area, (c)cracks [15].

2.3 Manual Analysis of EL Images

In the traditional method of finding defects in PV modules using electroluminescence (EL) images, a visual inspection is used to find and mark defects by hand. (Fig. 4) and Table 1 show that each subcell has a serial number to facilitate identification. The cells are then grouped according to their appearance. Defects are then classified based on their visual characteristics.

Table 1. Serial indexing of photovoltaic cells.

Serial N°									
A1	A2	A3	A4	A5	A6	A7	A8	A9	A10
B1	B2	B3	B4	B5	B6	B7	B8	B9	B10
C1	C2	C3	C4	C5	C6	C7	C8	C9	C10
D1	D2	D3	D4	D5	D6	D7	D8	D9	D10
E1	E2	E3	E4	E5	E6	E7	E8	E9	E10
F1	F2	F3	F4	F5	F6	F7	F8	F9	F10

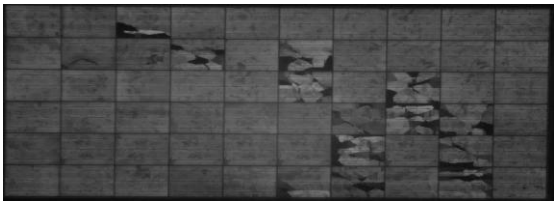

Fig. 4. EL imaging of polycrystalline Si cell (GEP dataset)

For example, subcell B2 has a finger break, while B3 has a scratch. More critical defects are observed in cells such as A3, B4, B6, C6, F6, D7, E7, F7, C8, D8, D9, E9, and F9, where severe cracks, branching fissures, and partial cell ruptures are clearly visible. The manual inspection method is simple to understand and use, but it is time-consuming, subjective and requires the expertise of a specialist; it is therefore not suitable for large-scale or real-time use. This highlights the importance of having automated and intelligent detection systems capable of analysing EL images accurately and consistently.

3 Methodology

3.1 Preprocessing and Dataset Preparation

3.1.1 The ELPV dataset

The standard set of electroluminescent (EL) image data referenced in the literature is identified as ELPV [16]. This unique collection contains 2624 EL image samples, each measuring 300 by 300 pixels, consisting of 8 bpp greyscale photographs of functional and faulty

solar cells. These photos were obtained from forty-four distinct solar modules displaying differing levels of deterioration. In ELPV [15], all extracted images were standardized in size and perspective. Furthermore, any potential distortion caused by the camera was eradicated before the retrieval of the solar cell. In the domain of photovoltaic electroluminescence (ELPV), the cell pictures originated from (mc-Si) or (pc-Si) photovoltaic modules.

3.1.2 Data Augmentation

Due to the limited size of the ELPV dataset, data augmentation was essential to enhance model generalization and reduce overfitting. Since the position and orientation of defects such as cracks and dark areas do not affect their classification, several geometric and photometric transformations were applied. These included random rotations (±20°), fixed rotations (90°, 180°, 270°), horizontal and vertical flipping, zooming (80%–120%), brightness variation, and contrast adjustment (Fig. 5). These transformations simulate real-world variations in image acquisition and increase the diversity of the training set. In some cases, cropping and shifting were used to emphasize local defect areas. Augmented images were manually reviewed to ensure label consistency, and the class balance between "defect" and "no defect" was maintained to stabilize model training

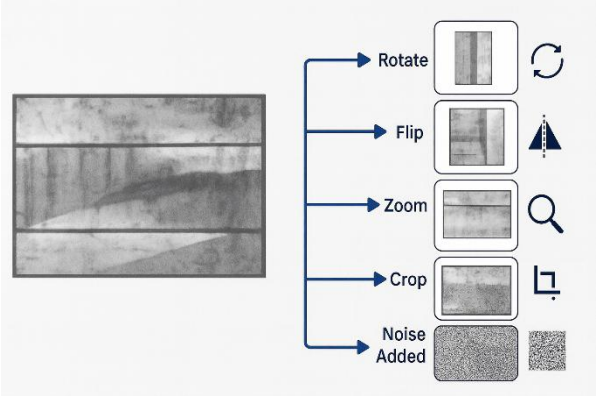

Fig. 5. Data augmentation of the ELPV dataset

3.2 Training the MobileNetV2 Model

To classify defects in EL images efficiently, we used MobileNetV2, a lightweight convolutional neural network optimized for low-resource environments. MobileNetV2 achieves high computational efficiency thanks to the use of depthwise separable convolutions,

which significantly reduce the number of parameters and floating-point operations compared to standard convolutions. This architectural choice makes MobileNetV2 particularly suitable for real-time and embedded photovoltaic inspection applications. The model was initialized with ImageNet-pretrained weights, and the top layers were replaced with a custom classification head for binary classification (defect vs. no defect) as shown in (Fig.6). This head comprised a global average pooling layer, a dense layer with ReLU activation, a dropout layer to mitigate overfitting, and a final sigmoid output layer. We optimized the last layers of MobileNetV2 to accommodate the characteristics of electroluminescence images. The model utilized the Adam optimizer with a learning rate of 0.0001 and applied binary cross-entropy as the loss function. Training was conducted for 50 epochs with a batch size of 32, employing early termination contingent on validation loss.

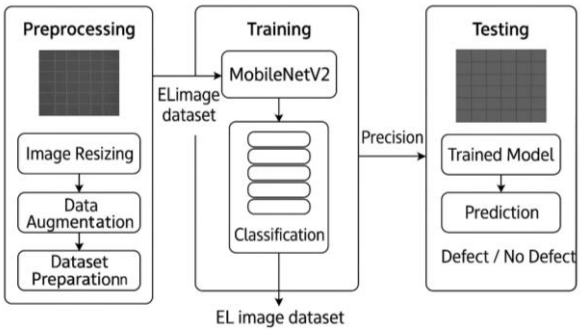

Fig. 6. Block diagram of the proposed MobileNetV2 architecture with final sigmoid output layer.

4 Results and discussion

This section presents and discusses the experimental results obtained using the MobileNetV2 model for binary classification of photovoltaic cell defects in electroluminescence (EL) images. The model performance is evaluated through accuracy and loss curves, as well as inference speed, to validate the effectiveness of the proposed approach.

4.1 Experimental Setup

From the original ELPV dataset containing 2624 images, a subset of 100 images (50 defective and 50 non-defective) was selected to conduct controlled experiments and evaluate the feasibility of the proposed approach under limited data conditions. The dataset was divided into three groups: 70% for training (70 images), 15% for validation (15 images) and 15% for testing (15 images).

We trained the model for 50 epochs using the Adam optimiser with a learning rate of 0.0001 and binary cross-entropy as the loss function. We used the early stopping method to stop training when the validation loss stopped improving.

4.2 Training and Validation Performance

As shown in (Fig. 7), the training accuracy quickly increased and stabilized around 98-100%, while the validation accuracy fluctuated between 80% and 85%, peaking at 85.4%. This indicates effective learning on the training data and reasonable generalization to unseen images, despite the limited dataset size. (Fig. 8) shows the corresponding training and validation loss curves. Training loss decreased consistently and approached zero, whereas validation loss showed more variability, a typical behavior when training with small datasets. Although a gap exists between training accuracy

(approximately 100%) and validation accuracy (approximately 85%), this behavior is expected when training on small datasets. Data augmentation and early stopping helped mitigate overfitting and ensured stable validation performance.

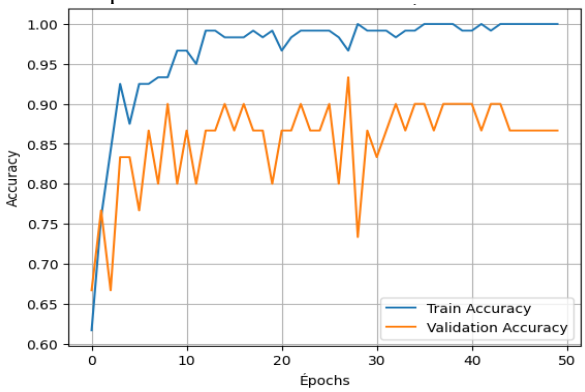

Fig. 7. Validation and training accuracy of the MobileNetV2.

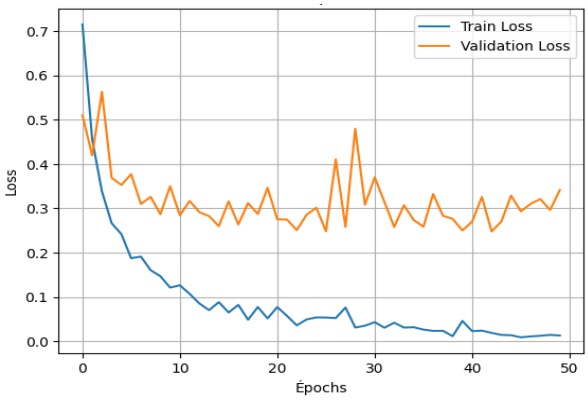

Fig. 8. Validation and training loss of the MobileNetV2.

4.3 Classification Results

The final MobileNetV2 model achieved a validation accuracy of 85.4%, and demonstrated an average inference time of 0.913 seconds per image. These results confirm that the model is capable of performing efficient and accurate classification, even with a small dataset. The use of data augmentation and fine-tuning significantly contributed to the model's ability to generalize

4.4 Performance comparison: MobileNetV2 vs. CNN

An in-depth comparison was made between the proposed framework based on MobileNetV2 and CNN in order to examine both prediction performance and computational efficiency. Table 2 shows that CNN has a slightly higher validation accuracy of 88.4% and an inference time of 0.889 seconds per image. Even though CNN had improved accuracy, it had a major computational problem: it took about 13 hours and 45 minutes to train it [17], making it much less useful for rapid deployment or real-time applications.
MobileNetV2, on the other hand, achieved an accuracy of 85.4% and an inference time of 0.913 s/image, while reducing training time to just 15 minutes. The low computational cost, with no major impact on accuracy, demonstrates the usefulness of MobileNetV2 for detecting defects in photovoltaic modules.
Overall, these results indicate that MobileNetV2 provides a strong deployment-oriented trade-off. Although its inference time (0.913 s/image) is slightly higher than some CNN-based methods (0.858–0.889 s/image), it remains compatible with near-real-time inspection. More importantly, MobileNetV2 significantly reduces the computational burden during training (15 minutes in our experiments versus several hours for conventional CNNs), and its lightweight design makes it more feasible for embedded or edge-based photovoltaic diagnostic systems.

Table 2. Performance Comparison Between CNN and MobileNetV2 Model.

Network Name	Method	accuracy (%)	Score (s/image)
Demirci et. al. [5]	CNN	82.6	0.858
Deitsch et.al. [18]	CNN	88.4	0.889
H.A.Al-Otum [19]	MobileNet-v2	74.5	0.5542
Proposed Mobilenetv2	MobileNet-v2	85.4	0.913

Although the proposed MobileNetV2 model exhibits a slightly higher inference time (0.913 s/image) than some CNN-based methods, the difference remains small and does not prevent near-real-time operation. Furthermore, its reduced training time and lightweight architecture improve deployment feasibility, especially for embedded or edge inspection scenarios.

5 Conclusion

This work presented a lightweight deep learning method based on the MobileNetV2 architecture that can automatically find defects in photovoltaic (PV) modules using electroluminescence (EL) images. The dataset used to train and test the model consisted of 100 images. Half of the images represented defective cells and the other half represented non-defective cells. Although the dataset was small, the model was able to achieve a validation accuracy of 85.4% with an inference time of 0.913 seconds per image, demonstrating that it is effective and can be used in real-time or near-real-time applications. The results show that MobileNetV2 could be a good way to reliably classify defects in EL images, especially when computational resources are limited. The application of data augmentation techniques and transfer learning played a key role in improving model performance and generalization.
This research contributes to the creation of intelligent, automated inspection systems and quality monitoring systems for the quality control of photovoltaic modules. These systems are particularly useful in industrial environments where speed and accuracy in decision-making are essential. Future studies will investigate the possibility of using larger data sets and combining them

with embedded technologies for on-site inspection of photovoltaic installations.

References

1. M. A. Green, E. D. Dunlop, J. Hohl-Ebinger, M. Yoshita, N. Kopidakis, and X. Hao, 'solar cell efficiency tables (version 56)', prog. photovolt. res. appl., vol. 28, no. 7, pp. 629–638, 2020, doi: 10.1002/pip.3303.
2. A. Anctil, C. W. Babbitt, R. P. Raffaelle, and B. J. Landi, 'cumulative energy demand for small molecule and polymer photovoltaics', prog. photovolt. res. appl., vol. 21, no. 7, pp. 1541–1554, nov. 2013, doi: 10.1002/pip.2226.
3. Y. Wang et al., 'adaptive automatic solar cell defect detection and classification based on absolute electroluminescence imaging', energy, vol. 229, p. 120606, aug. 2021, doi: 10.1016/j.energy.2021.120606.
4. W. Tang, Q. Yang, K. Xiong, and W. Yan, 'deep learning based automatic defect identification of photovoltaic module using electroluminescence images', sol. energy, vol. 201, pp. 453–460, may 2020, doi: 10.1016/j.solener.2020.03.049.
5. M. Y. Demirci, N. Beşli, and A. Gümüşçü, 'efficient deep feature extraction and classification for identifying defective photovoltaic module cells in electroluminescence images', expert syst. appl., vol. 175, p. 114810, aug. 2021, doi: 10.1016/j.eswa.2021.114810.
6. C. Schuss et al., 'detecting defects in photovoltaic panels with the help of synchronized thermography', ieee trans. instrum. meas., vol. 67, no. 5, pp. 1178–1186, may 2018, doi: 10.1109/tim.2018.2809078.
7. M. W. Akram et al., 'cnn based automatic detection of photovoltaic cell defects in electroluminescence images', energy, vol. 189, p. 116319, dec. 2019, doi: 10.1016/j.energy.2019.116319.
8. D.-M. Tsai, S.-C. Wu, and W.-C. Li, 'defect detection of solar cells in electroluminescence images using fourier image reconstruction', 9th int. meet. electrochromism, vol. 99, pp. 250–262, apr. 2012, doi: 10.1016/j.solmat.2011.12.007.
9. H. Munawer Al-Otum, 'deep learning-based automated defect classification in electroluminescence images of solar panels', adv. eng. inform., vol. 58, p. 102147, oct. 2023, doi: 10.1016/j.aei.2023.102147.
10. M. Sandler, A. Howard, M. Zhu, A. Zhmoginov, and L.-C. Chen, 'mobilenetv2: inverted residuals and linear bottlenecks', presented at the proceedings of the ieee conference on computer vision and pattern recognition, 2018, pp. 4510–4520.
11. C. Shorten and T. M. Khoshgoftaar, 'a survey on image data augmentation for deep learning', j. big data, vol. 6, no. 1, pp. 1–48, 2019.
12. T. Lai, B. G. Potter, and K. Simmons-Potter, 'electroluminescence image analysis of a photovoltaic module under accelerated lifecycle testing', appl. opt., vol. 59, no. 22, pp. g225–g233, aug. 2020, doi: 10.1364/ao.391957.
13. H. Munawer Al-Otum, 'classification of anomalies in electroluminescence images of solar pv modules using cnn-based deep learning', sol. energy, vol. 278, p. 112803, aug. 2024, doi: 10.1016/j.solener.2024.112803.
14. A. Korovin et al., 'anomaly detection in electroluminescence images of heterojunction solar cells', sol. energy, vol. 259, pp. 130–136, july 2023, doi: 10.1016/j.solener.2023.04.059.
15. C. Buerhop et al., a benchmark for visual identification of defective solar cells in electroluminescence imagery. 2018. doi: 10.4229/35theupvsec20182018-5cv.3.15.
16. C. Buerhop-Lutz et al., 'a benchmark for visual identification of defective solar cells in electroluminescence imagery', presented at the 35th european pv solar energy conference and exhibition, 2018, pp. 1287–1289.
17. S. Deitsch et al., 'segmentation of photovoltaic module cells in uncalibrated electroluminescence images', mach. vis. appl., vol. 32, no. 4, p. 84, 2021.
18. S. Deitsch et al., 'automatic classification of defective photovoltaic module cells in electroluminescence images', sol. energy, vol. 185, pp. 455–468, 2019.
19. H. A. Al-Otum, 'automatic defect detection and classification in electroluminescence images of pv cells using convolutional neural networks', 2023, ssrn. doi: 10.2139/ssrn.4422413.